https://doi.org/10.1595/205651324X17055018154113 *Johnson Matthey Technol. Rev.*, 2024, **68**, (1), 147–160

JOHNSON MATTHEY
TECHNOLOGY REVIEW

technology.matthey.com

# Benchmarking Stability of Iridium Oxide in Acidic Media under Oxygen Evolution Conditions: A Review: Part II

## Investigation of catalyst activity and stability *via* short term testing

**James Murawski*, Soren B. Scott, Reshma Rao**
Department of Materials, Imperial College London, Exhibition Road, London, SW7 2AZ, UK

**Katie Rigg, Chris Zalitis, James Stevens, Jonathan Sharman**
Johnson Matthey, Blount's Court, Sonning Common, Reading, RG4 9NH, UK

**Gareth Hinds**
National Physical Laboratory, Teddington, Middlesex, TW11 0LW, UK

**Ifan E. L. Stephens**
Department of Materials, Imperial College London, Exhibition Road, London, SW7 2AZ, UK

***Email:** j.murawski18@imperial.ac.uk

**PEER REVIEWED**

Received 10th February 2023; Revised 15th May 2023; Accepted 22nd May 2023; Online 23rd May 2023

Part I (1) introduced state-of-the-art proton exchange membrane (PEM) electrolysers with iridium-based catalysts for oxygen evolution at the anode in green hydrogen applications. Aqueous model systems and full cell testing were discussed along with proton exchange membrane water electrolyser (PEMWE) catalyst degradation mechanisms, types of iridium oxide, mechanisms of iridium dissolution and stability studies. In Part II, we highlight considerations and best practices for the investigation of activity and stability of oxygen evolution catalysts *via* short term testing.

## 1. Practical Considerations for Oxygen Evolution Reaction Stability Testing

### 1.1 Experimental Setup

In this section, we will focus primarily on the test conditions and design when using a rotating disc electrode (RDE) setup for accelerated degradation testing of catalyst stability. However, many of these considerations are relevant to other setups such as gas diffusion electrode (GDE) cell designs. Before testing it is best to ensure the electrochemical cell that is being used has been thoroughly cleaned of any organic or inorganic contaminants by using a suitable oxidising acid bath alongside repeated rinsing and boiling in ultrapure (Type 1, 18.2 MΩ cm) water.

For oxygen evolution reaction (OER) studies often a counter electrode of platinum wire/mesh is utilised, preferably of an order of magnitude larger surface area than that of the working electrode in order to not limit the reaction occurring at the working electrode (2). Some studies involving non-platinum group metal catalysts can be concerned about the presence of platinum resulting in enhanced performance. This can be mitigated by the use of carbon as counter electrode; separating the counter electrode from the working electrode with a perfluorosulfonic acid (PFSA) membrane or glass frit in order to minimise crossover or a combination of the two. Although for OER, dissolved platinum is likely to redeposit on the cathode (counter electrode), as observed for hydrogen evolution reaction studies and is therefore unlikely to interfere with the performance of the working electrode. It is worth noting that PFSA membranes will not completely

stop platinum crossover as demonstrated in both wet cell (3) operational PEMWE systems (4). For more comprehensive best practices on the use of RDE we refer the reader to recent work by Alia *et al.* which suggests standardised procedures and practices for acidic media OER studies using RDE (5).

## 1.2 Electrochemical Procedure Considerations

### 1.2.1 Potential Limits for Activity and Stability Measurements

When selecting potential limits for cycling or step experiments, the upper potential limit has to be positive enough that a degradation rate can be observable and that different catalysts can be ranked over the time of the experiment; on the other hand, it should not be so positive for measurement quality and validity. Excessive bubble formation that occurs at high current density can cause noise in the data and also alternative degradation mechanisms such as detachment that do not necessarily occur in a real system. Exceeding the potential that a real system operates at runs the risk of accelerating other alternative degradation mechanisms (6). The other consideration is that for assessment of very stable $IrO_x$ catalysts some inductively coupled plasma-mass spectrometry (ICP-MS) systems may struggle with detecting lower quantities. It is possible then that an increased potential limit may be more appropriate to distinguish dissolution losses. The lower limit should be in a region of no OER activity; while 1.2–1.4 $V_{RHE}$ is sometimes used (7), studies have been conducted on varying limits. It has been suggested that going below 0.9 $V_{RHE}$ results in enhanced (8, 9) and therefore more observable, degradation of the anode catalyst. In this case a lower limit of 0.4–0.6 $V_{RHE}$ could be considered, although this is unlikely to be experienced by a PEMWE system regularly outside of start-up/shutdown.

### 1.2.2 Background/Double Layer Correction

One of the major aspects of processing activity measurement data, particularly from cyclic voltammetry (CV), aside from compensating for *iR* drop, is accounting for current associated with the double layer capacitance. Conventionally, this would be done by subtracting the current from a region where there is no faradaic activity (i.e. 0.4–0.6 $V_{RHE}$ for metallic platinum). However, for $IrO_x$ this is made slightly more complicated by the fact that the cyclic voltammogram of $IrO_x$ has no clear double layer region (see **Figure 1(b)**). Instead, capacitance current can be mitigated by low scan rate (see **Figure 1(a)**) or taking the average of the anodic and cathodic scans, though neither approach is perfect. Ultimately, this motivates the importance of not entirely relying on

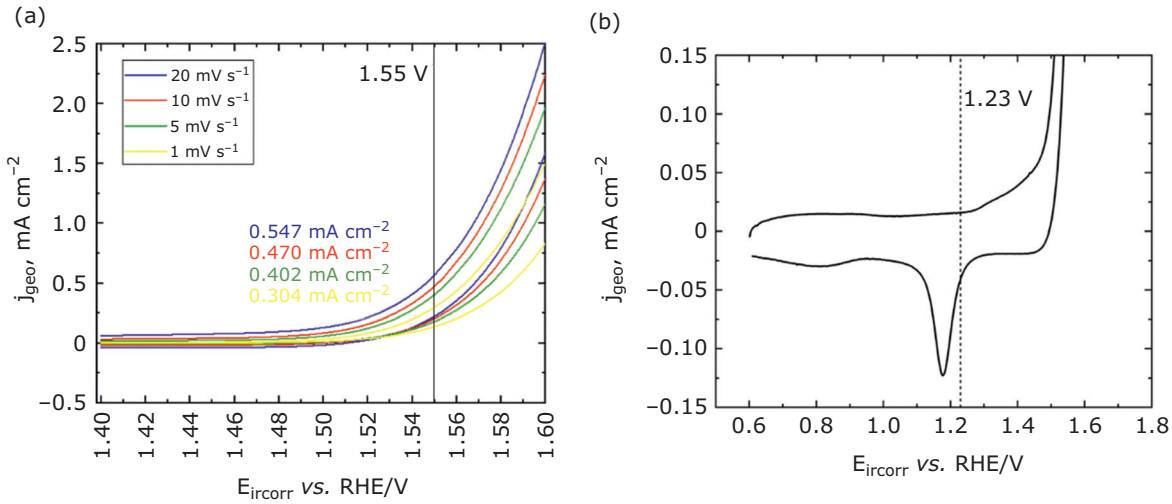


Fig. 1. CV data of commercially available 10 µg $cm^{-2}$ $IrO_x$ obtained from Alfa Aesar on gold insert in 0.1 M $HClO_4$: (a) CV of $IrO_x$ at different scan rates with activity value at 1.55 V with no double layer correction; (b) CV of $IrO_x$ with no clear non-Faradaic double layer region because of various features visible on the anodic and cathodic sweep

CV but also using constant potential measurements for activity measurement (10).

## 1.3 pH and Electrolyte Effects

Assessing the pH that the catalyst is exposed to is difficult in PEMWE systems as the proton conducting ionomer membrane (i.e. Nafion®), that functions as the electrolyte, that is in direct contact with the anode and cathode catalyst by itself is transparent to pH (11). However, Nafion® is a superacid catalyst with pKa ~–6 which results in the ability to conduct protons with ease (12). Overall, this results in the catalyst in direct contact with the membrane being in what is considered a very acidic environment, but direct determination of the pH at the catalyst is challenging.

The electrolyte most commonly used for aqueous model testing of OER catalysts is 0.1 M high purity perchloric acid in ultrapure (Type 1 18.2 MΩ cm) water. This is because of the relative independence of catalytic activity from concentration of perchloric acid (13). 0.05 M sulfuric acid is also commonly used. Work by Arminio-Ravelo *et al.* on electrolyte effects on iridium-based nanoparticles for OER has explored both perchloric acid and sulfuric acid at various concentrations (0.05 M, 0.1 M and 0.5 M), showing that sulfuric acid reduced the catalytic activity with increasing concentration, while activity was relatively independent of concentration in perchloric acid (13). The reduction in activity was put down to strong adsorption of sulfate and bisulfate anions interfering with the oxidation of iridium, as opposed to the weaker adsorption of perchlorate anion (13). The concentration of 0.1 M perchloric acid is a balance between reduced uncompensated resistance with higher electrolyte concentration *versus* the cost of using a higher quantity of stock perchloric acid as well as possible negative effects on activity. However, the effect of choice of electrolyte and concentration on dissolution could be of greater interest in future model studies especially considering results that show that higher pH results in reduced observable iridium dissolution both in membrane electrode assembly (MEA) and aqueous model systems (AMS) (14).

Localised acidity is also suggested (14, 15) as another major factor in the disparity between catalyst lifetimes measured in MEA and AMS such as RDE and SFC. Experimental evidence from MEA level studies (14) showed that compared to operation in deionised water, operation in 0.1 M sulfuric acid resulted in a reduction of stability by over an order of magnitude. This compensates for the majority of the discrepancy, however MEAs run in 0.1 M sulfuric acid still demonstrated greater stability than in the corresponding AMS, indicating that greater acidity, alongside other affects (16), is a cause of faster dissolution in the model systems. The presence of anions ($ClO_4^-$, $HSO_4^-$, $SO_4^{2-}$) in model systems of RDE and SFC can help stabilise dissolved species of iridium, which are usually quite unstable due to the thermodynamic stability of undissolved species in most conditions (17). The increased flow of electrolyte away from the electrode, alongside the stabilisation of dissolved iridium, also allows the dissolved iridium to be moved away from the electrode before it is able to redeposit. In a MEA the restricted flow of the water at the catalyst surface (18) and the lack of stabilising anions, outside of the PFSA membrane, could result in: (i) a greater proportion of iridium being redeposited on the catalyst or across the membrane; and/or (ii) dissolution being less favourable due to a higher local concentration of dissolved iridium, which is not transported away. Further studies on both pH and flow effects on stability in model systems could be worthwhile in determining discrepancies from real systems.

Acidity has also been studied using online ICP-MS measurements, see **Figure 2** and the results support the idea that the localised pH is a contributing factor to the overall dissolution. The highest dissolution rate was observed at the baseline of pH 1 with lower dissolution rates

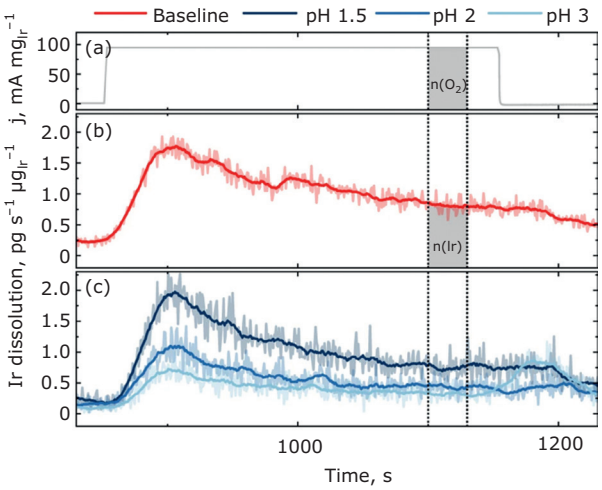


Fig. 2. The effect of pH change of electrolyte on dissolution of IrOx catalyst indicating higher dissolution at lower pH: (a) current density profile; (b) baseline measurement 0.1 M $HClO_4$; (c) iridium dissolution. Reproduced from Knöppel *et al.* (14), under CC-BY 4.0 international license

(greater S-numbers) seen for both samples tested at pH 1.5, pH 2 and pH 3. Therefore, while the reduction in electrolyte concentration gives a small observable reduction in activity (13) it accounts for some, see MEA comparison Table IV in Part I (1), of the lower dissolution rates due to reduced stabilisation of dissolved iridium species as observed in MEA testing (14).

## 1.4 Effects of Conditioning Gas

In a MEA setup the anode catalyst would generally be in an oxygen-saturated environment due to oxygen evolution. While many OER studies have been conducted in both saturated argon environments and saturated oxygen environments, there have not been many investigations into the impact of conditioning gas in stability measurements. Scott and Rao *et al.*, using electrochemistry mass spectrometry (EC-MS) and isotopic labelling, observed no change in rate of $H_2{}^{18}O$ oxidation to $^{18}O_2$ on ruthenium oxide when the electrolyte was saturated with $^{16}O_2$, but this comparison was only made at low current densities below the threshold for bubble formation (19). Similarly, a study in alkaline environment demonstrated that for activity measurements there is either no or negative effect on OER activity in an oxygen saturated environment (20). The study could not confirm whether this effect was the result of a change in the state of the surface or as a result of enhanced bubble formation due to the higher oxygen content of the saturated electrolyte. This enhancement would tie in with previously mentioned studies conducted on gas blinding and offers one potential method for identifying the cause of performance loss, by observing a less significant decrease in activity in the presence of a sonic horn (see Section 2.1.2 in Part I (1)) (21).

Testing conducted for this review with the perspective to resolve the issue is shown in **Figure 3**. Current density is shown at three different hold potentials in different conditioning gases. The conditioning gas appears to have little effect on performance in comparison to performance loss due to gas blinding by evolved oxygen, or the catalyst surface oxide change (22) (seen as a reduction in current density between each run). It is likely that oxygen being evolved saturates the region local to the electrode and the only effect of oxygen saturation is to make it slightly harder for the oxygen to dissolve, as seen in alkaline OER studies (20). This performance loss is recoverable by regeneration *via* low potential cycling as well as other methods that have been proposed, such as purging with argon at open circuit voltage (OCV) (23).

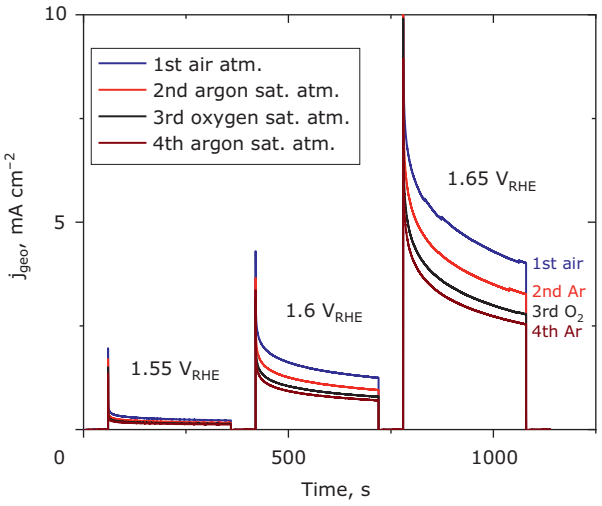


Fig. 3. Work conducted for this review to confirm the effect of conditioning gas on catalyst performance. The results show that saturation of atmosphere on 10 µg cm$^{-2}$ $IrO_x$ obtained from Alfa Aesar during short term potential holds (1.55 V, 1.6 V and 1.65 V *vs.* RHE) in 0.1 M $HClO_4$. After repeated 5 min holds at multiple potentials with 1 min potential holds at 1.3 V in between gas was changed and allowed to saturate solution for minimum of 15 min. Samples were not allowed to drop below 1.2 V between holds by conducting 1.3 V holds during gas changes

## 1.5 Temperature

Typically, PEMWE systems will operate at 60–80°C, with AMS usually being tested at room temperature. This is due to the increasing complexity required for higher temperature measurements over the longer time periods involved in AST in AMS to avoid evaporation of water, which could lead to changes in the electrolyte concentration. The increasing temperature would be expected to increase the activity in line with Arrhenius effects but also increases the instability of the catalyst by increasing the rate of dissolution, especially as most degradation routes couple the activity and degradation reaction (6). While almost all PEMWE MEA studies are conducted at elevated temperature there have been relatively limited studies of the effects of temperature on dissolution or electrochemical performance degradation. Comparison studies between MEA and RDE conducted at 80°C showed that at low overpotentials, 1.45–1.55 V there is comparable

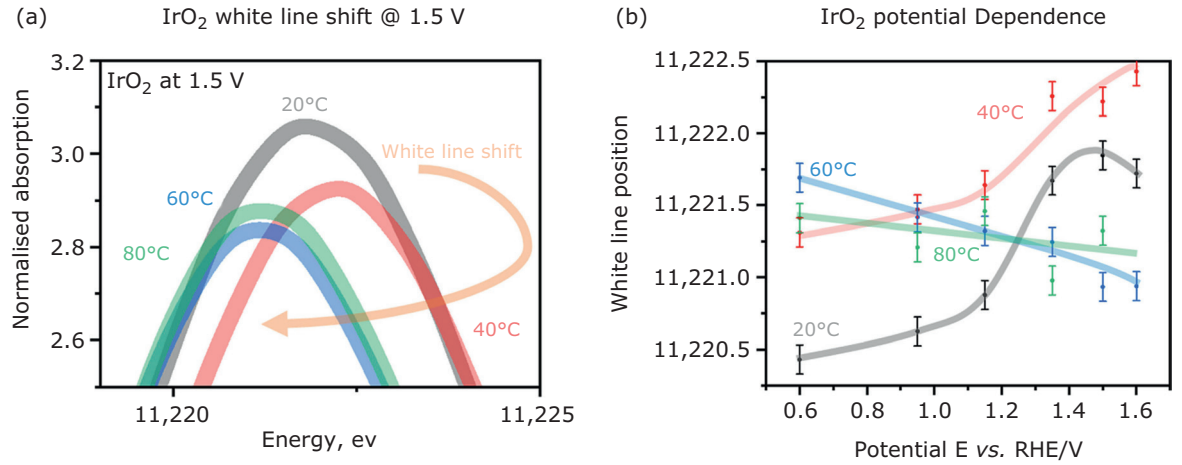


Fig. 4. Results from using XANES to explore white line shift of $IrO_2$ at different temperatures 20°C (grey), 40°C (red), 60°C (blue) and 80°C (green) showing: (a) white line shift of $IrO_2$ at 1.5 V; (b) potential dependence of white line position. Reproduced from Czioska *et al.* (25), under CC BY-NC 4.0 international license

activity between the two systems when the results have been normalised to mass loading (24). This contrasts to the observed higher stability ratio in MEA systems (14). Ultimately, while comparable performance has been demonstrated in the low current density region (24), there is still some question about the extent that temperature affects degradation beyond improving activity and thus reducing the overpotential required to meet the same current density.

Recent work by Czioska *et al.* utilised *operando* X-ray absorption spectroscopy (XAS) to investigate the effects of temperature and potential on iridium oxide oxidation. They observed a white line shift to lower energies when going from operational lower temperature (20–40°C) to higher temperature (60–80°C) at 1.5 V indicating overall a more reduced surface, see **Figure 4(a)** (25). The reduction, seen as the decreasing slope in **Figure 4(b)**, at higher temperature and potentials was attributed to the formation of a greater number of oxygen vacancies (26) associated with higher flux of oxygen. Increasing white line position was observed with lower temperature (20–40°C) measurements in line with oxidation of the surface, although for 20°C a reverse is seen at 1.6 V that requires further investigation.

## 1.6 Electrode Substrate

The substrate on which the OER catalyst is deposited has to meet the criteria of: (i) high conductivity; (ii) high stability; and (iii) low activity. Choices are limited. The substrates that are often used in model testing are often different to those used in MEA setups due to cost or ease of working with the material. Geiger *et al.* investigated the suitability of several common backing substrates for OER in accelerated ageing studies in model systems (RDE), including gold, glassy carbon (GC), fluorine-doped tin oxide (FTO) and boron-doped diamond (BDD) (27), highlighting gold and BDD as the best candidates. The initial factor that is important to consider when selecting or designing a substrate is that the conductivity of the substrate is sufficient to avoid unnecessarily high circuit resistance. Most commercially available disc inserts used in RDEs meet this requirement, but it must be considered if designing a novel backing substrate. Stability under OER is the second consideration. GC, a common substrate that is sometimes used in activity measurements, is unsuitable due to corrosion, although typically in the high potential ~1.9 $V_{RHE}$ region (28, 29). In addition, even stable substrates such as gold can undergo dissolution if the catalyst loading is very low, as seen by Zheng *et al.* (30). The final condition is activity of the substrate for the OER. Some substrate materials such as gold can have a small but observable activity toward OER at higher overpotentials in comparison to $IrO_x$. Another promising strategy for substrates for stability testing is to coat a titanium disc insert with a thin layer of platinum. This resembles a typical commercial PEMWE, where platinised titanium mesh is used as the PTL on the anode side.

## 1.7 Accounting for Artifacts: Gas Blinding, Surface Oxide Changes and Activity Regeneration

Some experimental works have utilised an inverted or angled setup using an RDE, allowing the planar face of the electrode to be facing up and thereby removing one of the limitations for bubble detachment from the surface. However, this requires additional consideration for the operation of the cell to prevent against electrolyte leakage. It is worth pointing out that while this approach may assist in the removal of large bubbles that block the surface, it will not accelerate removal of oxygen bubbles in the micropores of the deposited catalyst layer (21). Over the course of long-term AST, cavitation and further gas formation can result in the removal of macro-bubbles. A more significant issue occurs during activity measurements where surface blockage over short periods of time can give an unreliable measurement of performance. When conducting activity tests, it has been suggested (23) that holding the electrode at OCV for 30 min in saturated argon electrolyte might remove some of the effects of gas blinding caused by evolved oxygen; however, upon cycling the activity in the oxygen evolution region will continue to decrease. Alternatively, this protocol could be reversing the partial deactivation observed due to surface oxidation or structure changes (22). Work by Trogisch *et al.* (31) also indicate that all catalyst layers will undergo gas blinding and predict that catalysts with different properties such as porosity, which can affect gas transport, will perform differently in AMS to MEA systems. While this was shown to be the case for all catalyst loadings, minimising catalyst layer thickness <30 μg $cm^{-2}$ will reduce the proportion of the overall catalyst layer that is shielded *versus* that is accessible, albeit the artifact will still be present.

## 1.8 Electrochemical Surface Area Measurements

A general challenge when dealing with metal oxide electrocatalysts is accurately determining the electrochemical surface area (ECSA). The common techniques used for ECSA determination of platinum, such as hydrogen underpotential deposition or carbon monoxide (CO) stripping, are not possible with metal oxides. In the case of hydrogen underpotential deposition, the sites at which the hydrogen would normally adsorb are not present in the $IrO_x$ structure (or in metal oxides more generally), so no hydrogen adsorption/desorption peaks are seen. For CO stripping it is challenging to deconvolute the CO stripping peaks due to the weak or no adsorption of CO on metal oxides (32). BET is often used as an approximation for ECSA as for unsupported metal oxides the ECSA and physical surface area should provide similar values (33). Although this is dependent on making a catalyst layer with a specific loading and using that weight alongside the BET surface area value as an approximation, it also cannot be used to measure change of ECSA during electrochemical measurements. The following methods are used instead (see **Table I**).

### 1.8.1 Double Layer Capacitance

The most commonly used technique for determination of ECSA is *via* measurement of the double layer capacitance by conducting several CVs at different scan rates over a region that usually includes 1.1–1.2 $V_{RHE}$ where there should be no

**Table I Methods for ECSA Determination of Metal Oxides Including Normalisation Factor for the Various Ir/$IrO_x$ Including Roughness Factor (RF)**

| Method | Normalisation factor | Type of $IrO_x$ for factor | Conditions |
|---|---|---|---|
| **CO stripping (Ir metal only) (34–36)** | 358 μC $cm_{Ir}^{-2}$ | Polycrystalline Ir, RF: 1.6 | 0.6 $V_{RHE}$ upper limit |
| **$C_{DL}$ double layer capacitance (CV) (37, 38)** | 350 μF $cm_{Ir}^{-2}$ | | CV @ 1.1–1.2 $V_{RHE}$ |
| **$C_{DL}$ double layer capacitance (CV) (39) (alkaline)** | 130 μC $cm_{Ir}^{-2}$; 90 μC $cm_{Ir}^{-2}$ | $IrO_2$ (100); $IrO_2$ (110) | 0.1 M KOH |
| **$C_a'$ adsorption capacitance (EIS) (41)** | 135 ± 25 μF $cm_{Ir}^{-2}$ | $IrO_x$ from Ir (111) single crystal RF: 1.01 | EIS @ 1.59 $V_{RHE}$; 0.1 M $HClO_4$ |
| **$C_a'$ adsorption capacitance (EIS) (41) (alkaline)** | 172 ± 35 μF $cm_{Ir}^{-2}$ | $IrO_x$ from Ir (111) single crystal RF: 1.01 | EIS @ 1.68 $V_{RHE}$; 0.1 M KOH |
| **Mercury underpotential deposition (36)** | 138.6 μC $cm_{Ir}^{-2}$ | Polycrystalline Ir, RF: 1.3 | 1 mM $HgNO_3$ in 1 M $HClO_4$ |

activity in most cases (32). Dividing the measured capacitance by the specific capacitance value for $IrO_x$ (350 μF $cm^{-2}$) gives the ECSA (37, 38). This technique requires several assumptions: (i) double layer capacitance and resulting specific capacitance, is unchanging from one $IrO_x$ surface to another; (ii) there is no contribution from adsorption capacitance or intercalation of protons into the bulk; (iii) there is a clearly defined surface area. In practice these assumptions can be questioned for metal oxides. Even on single-crystal platinum values of specific capacitance can vary by up to a factor of 1.8 (10) and a much greater variation of surface specific capacitance is expected for $IrO_x$ surfaces.

### 1.8.2 Adsorption Capacitance

Alternatively, a more recent method that has been studied is the use of electrochemical impedance spectroscopy (EIS) to determine a capacitive value by modelling the measured impedance response (40). The proposed differential adsorption capacitance ($C_a'$) is obtained from fitting the EIS spectrum at kinetically active potentials to obtain the plateau adsorption capacitance $C_a$ value. This is compared to values of $C_a'$ obtained from capacitance in a model surface where ECSA can be determined by atomic force microscopy (AFM) and/or $CO_{ads}$ stripping voltammetry of thin films. For $IrO_x$ (obtained from cycling an Ir (111) single crystal) in 0.1 M $HClO_4$ at 1.59 $V_{RHE}$, the specific adsorption capacitance has a value of 135 ± 25 μF $cm^{-2}$ (41). While there is strong empirical evidence for this correlation with ECSA, the fundamental explanation of the adsorption capacitance is more open to interpretation, given the difficulty in assigning fundamental features to EIS data with certainty. In addition to this, there remain questions about how significantly the specific adsorption capacitance may vary within different types of $IrO_x$ (42). The simplicity and speed of conducting EIS measurements allow for this to be quite easily coupled with existing protocols for ECSA tracking, as EIS will often already be conducted to obtain uncompensated resistance.

### 1.8.3 Mercury Underpotential Deposition

Mercury underpotential deposition (36) has also been used to investigate ECSA of metal oxides. This process involves the underpotential deposition of mercury in a 1 mM mercury nitrate in 0.1 M perchloric acid solution during CV. A comparison of the charge under the anodic peak for desorption of the mercury in the 1 mM mercury nitrate solution is made with the results in pure 0.1 M perchloric acid, which is used as a baseline. A value of 138.6 μC $cm_{Ir}^{-2}$, obtained *via* earlier studies (43) on polycrystalline iridium, is used as a conversion factor. The results from Alia *et al.* for the mercury underpotential deposition correlated with BET results for the tested iridium and $IrO_x$ catalysts. The results also appear to show similar values to that obtained by other techniques (see **Table I**). The presence of 1 mM mercury nitrate complicates testing, likely requiring change of electrolyte between performance and stability testing or alternatively conducting the measurement separately.

## 1.9 Accelerated Stress Test Protocol

Taking into account all the above considerations, we provide a general flow chart (**Figure 5**) that tries to cover these points above to outline a procedure. As there are still many unknowns this is not intended as a definitive protocol but instead to highlight various avenues that can be taken when selecting an AST. We also would refer to the various techniques in Table II in Part I (1) and practical studies referenced in Table III in Part I (1). While the primary focus is AMS it should be noted that for CCM testing additional conditioning steps and adaptation would be needed, for example flowing water through cell for several hours to allow for swelling of membrane and removal of ionic contaminates in or on the membrane. We also indicate the minimum number of samples that should be taken for ICP-MS monitoring of dissolved iridium species. In addition to the AST we also recommend the measurement of dissolution over a short period of constant operation to obtain a S-number (15) as well as monitoring of this value after AST to monitor how extended periods of degradation affect catalyst dissolution.

## 2. Future Technique Development

In the future, other methods for investigating novel OER catalysts could be explored that better simulate MEA testing but on a much smaller scale. Alternatively, the development of approaches to counter or limit the issue of microbubble formation in RDE testing would be desirable given the widespread use of the technique.

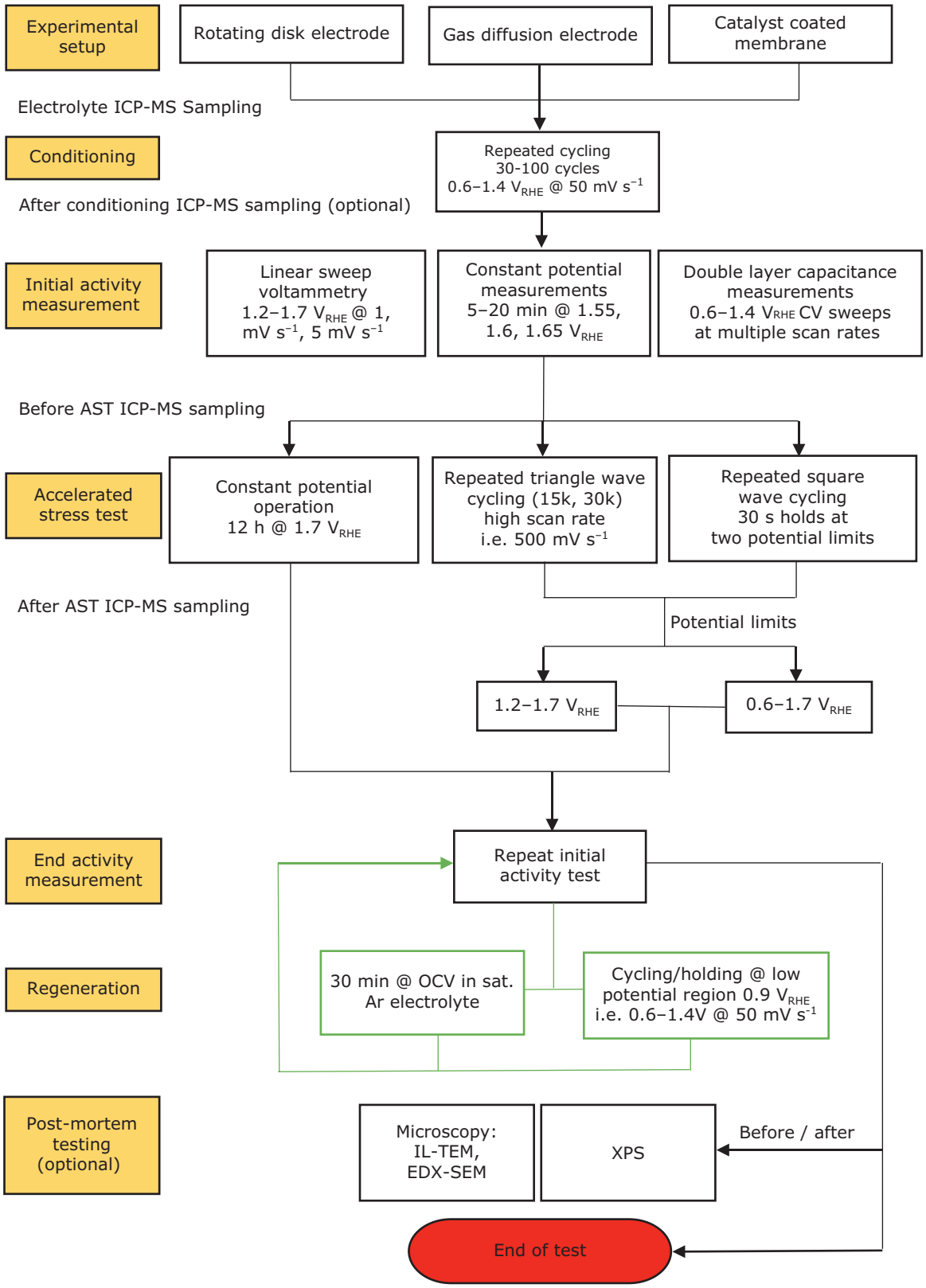


Fig. 5. AST activity and stability protocol

## 2.1 Gas Diffusion Electrodes, Microelectrodes and Convergence with MEA systems

GDEs could be considered for future small-scale three-electrode testing setups such as the floating electrode (44) or other GDE arrangements (45, 46) that form miniature half cells with catalyst deposited on a GDL allowing for higher mass transport. To date, these techniques have been used primarily for oxygen reduction and hydrogen oxidation/evolution studies where higher current density can be achieved as they are not limited by the same mass transport of reactants seen in RDE studies. Mass flow of reactant generally is not considered particularly problematic for activity in OER catalysis; however, shortening the distance of travel or increasing the rate that the oxygen flows away from the surface is desirable to minimise the amount of gas blinding of the catalyst layer.

While moving further away from real systems, microelectrodes (47) have been used to achieve high current densities during studies of OER materials due to improved mass transport and increasing the potential at which bubbles form. Cavity microelectrodes (48–50) allow for electrochemical measurements of powdered materials so can be used for the study of nanoparticle catalysts. These have been used for the study of $IrO_x$ materials; however, only to moderate geometric current densities (50) of ~40 mA $cm_{geo}^{-2}$ @ 1.65 $V_{RHE}$ albeit with significantly lower loading. Some studies indicate that bubble formation is still a problem due to the slightly larger microelectrode (50–60 µm in diameter (48)) and much higher surface area when accounting for all the catalyst in the cavity.

Alternatively, there have been attempts to integrate both the RDE and the CCMs that are used in MEA cell testing. This modified rotating disc electrode (MRDE) (51) allows for testing at high current density >2 A $cm^{-2}$ without rotation while retaining the small-scale setup of an AMS. This technique was also used to investigate the regeneration of activity, showing that regeneration may also be a factor in CCM testing when placed in a hybrid AMS as well as possibly in full cell systems more generally.

## 2.2 Increased MEA Studies *via* More Accessible Testing

There is also increasing acknowledgement of the need for more in-depth MEA level studies (14, 52) of suitable catalysts to ensure that catalysts perform as expected in a device and that other properties, such as conductivity and layer formation can be tested (53). MEA data should also be used to make comparisons with model setups to further optimise them for screening and fundamental studies. This is important as CCM testing includes many other factors such as membrane deformation into the PTL and chemical degradation causing membrane thinning, both of which can complicate the data and make it hard to isolate the effect of the catalyst stability. In this sense CCMs have been shown to need >1000 h (54) before they become stable to do these measurements, which is very constrictive for catalyst screening.

MEA systems can be difficult or costly for research groups to establish and maintain. Conversely, the development of cost-effective three-dimensional printed cell designs that replicate operation of a PEM MEA can allow for academic laboratories to more easily test promising candidates under realistic conditions (55). The two primary reasons for the continued importance of these AMS are the large increase in material required between RDE ink (approx. 5 mg) and MEA ink (approx. >1 g) and the difficulties deconvoluting effects of individual components in MEA experimental setups such as specifically measuring anode catalyst degradation. The development of these types of small scale, easy to prepare CCM setups allows for more widespread MEA level research to be conducted.

In addition, like wet cell testing, work on standardising protocols is also needed to allow better cross laboratory comparison. Although in its infancy, there have been efforts to normalise the data collected with the release of the EU harmonised degradation protocol (56), while several groups have also released their protocols (14, 54, 57).

# 3. Summary

## 3.1 Where Should the Field be in 10 Years' Time?

In this review we have split the future research needs into six distinct but not exhaustive areas outlined below.

**Increase iridium utilisation:** within 10 years ideally a large headway will have been made to increase iridium utilisation (roughly 20–40 times reduction in loading, improvement of utilisation) from the current generation systems (58–60), to allow for larger scale ($TW_{H2}$ total capacity >~100 GW $yr^{-1}$ $tonne_{Ir}^{-1}$) implementation of PEMWE technologies. To achieve the larger scales, the amount of iridium

will need to be thrifted, possibly by the use of mixed oxides to increase catalyst performance. Stability testing at both the AMS and MEA levels will be required to screen potential catalysts as it will be key to maintain stability while improving activity, limiting many of the potential candidates for mixing.

**Transition to high mass transport AMS:** to overcome the limitations of the RDE and general artefacts associated with AMS, a transition to high mass transport systems could be considered (8, 44, 45). The challenge that alternative systems face is that they need to be implemented in a way that means they can be used 'out the box' like many RDE systems. To achieve this, basic commercialisation of these high mass transport techniques is required to enable easier setup for research and industry groups that want to utilise them.

**Standardisation of stability procedures and metrics:** standardisation of stability measurements for comparison of catalysts utilising concepts such as the stability number should enable easier comparison between different catalysts allowing for more efficient screening of novel catalysts. Understanding if the stability number changes with long periods of constant operation or during different types of load cycling could enable improved understanding of how catalysts will operate over the longer time periods expected of commercial systems. In addition, a degree of standardisation of the protocols (7–9) themselves, particularly AST alongside justification of the condition could aid in the comparison of newly developed catalysts.

**Improved mechanistic understanding of dissolution process:** steps have been made to look into the degradation mechanism as well as experimental probing of both potential intermediate species (6) i.e. $IrO_3$ and also the relation between iridium dissolution and lattice oxygen evolution (61). Going forward establishing what are the dominant degradation pathways and whether these are the same for different catalysts could be key to both designing suitable AST and tuning longer lifetime catalysts.

**Electrochemical surface area measurements of metal oxides validation:** while there are techniques for looking at ECSA of metal oxides, they either are impractical to perform while conducting regular activity and stability measurements or there are questions about the fundamental explanation of the value that is used (41, 40). Further validation of different types of $IrO_x$ utilising comparison between these techniques could help bring more confidence to the values obtained.

**Contamination effects on stability:** the extent that contaminants can accelerate degradation have not been particularly well investigated but could result in alternative degradation pathways and performance losses. This becomes even more relevant if lower quality water is considered for operation to reduce overall operational costs.

## 3.2 Conclusion

In conclusion, RDE and other half-cell setups are unsuitable for directly predicting the catalyst lifetime in MEA setups (7, 15) due to the disparities that are seen between model and PEMWE systems. These model systems can still be useful when testing candidate catalysts to take to MEA testing as long as the limitations are understood and mitigated against where possible. RDE measurements will likely remain the most common tool available to electrochemists for small scale catalyst studies until better alternatives are developed and more widely implemented. In addition, the use of *in situ* and *ex situ* techniques which directly probe degradation, such as ICP-MS, is necessary to aid in comparison of catalyst stability and to further support electrochemical measurements for both benchmarking and fundamental studies.

Alternative methods such as novel systems with better gas diffusion should also be used to test whether improved mass transport away from the working electrode minimises gas blinding. Such gas diffusion systems also more closely simulate the GDLs present in MEA setups. Future stability studies of $IrO_x$ should also be combined with fundamental studies, where possible, to look at the mechanism for iridium dissolution which still is not fully understood. In addition, studies are required to identify whether trends in activity and stability are maintained in MEA setups. Further studies establishing correlations between RDE systems and working MEA systems (14, 24) could validate use of conventional techniques for screening studies as well as aid in the development of new acid-stable OER catalysts.

## Acknowledgement

We would like to acknowledge the Engineering and Physical Sciences Council for an industrial CASE studentship with contributions from National Physical Laboratory and Johnson Matthey. This work was partly supported by the National Measurement System of the UK Department of Business, Energy & Industrial Strategy. SBS was also supported in part by by the Marie Sklodowska Curie Actions and Iberdrola Group, Grant Agreement №101034297.

 

## Glossary

| | |
|---|---|
| AFM | atomic force microscopy |
| AMS | aqueous model system |
| AST | accelerated stress test |
| ATO | antimony-doped tin oxide |
| BDD | boron-doped diamond |
| BET | Brunauer-Emmett-Teller |
| CCM | catalyst-coated membrane |
| CV | cyclic voltammetry |
| DEMS | differential electrochemical mass spectrometry |
| EC-MS | electrochemistry mass spectrometry |
| ECSA | electrochemical surface area |
| EDX | energy dispersive X-ray |
| EELS | electron energy loss spectroscopy |
| EIS | electrochemical impedance spectroscopy |
| EQCM | electrochemical quartz crystal microbalance |
| FTO | fluorine-doped tin oxide |
| GC | glassy carbon |
| GDE | gas diffusion electrode |
| GDL | gas diffusion layer |
| ICP-MS | inductively coupled plasma-mass spectrometry |
| IL-TEM | identical location transmission electron microscopy |
| MEA | membrane electrode assembly |
| MRDE | modified rotating disc electrode |
| OCV | open circuit voltage |
| OER | oxygen evolution reaction |
| OLEMS | online electrochemical mass spectrometry |
| PEM | proton exchange membrane |
| PEMWE | proton exchange membrane water electrolyser |
| PFSA | perfluorosulfonic acid |
| PTFE | polytetrafluoroethylene |
| PTL | porous transport layer |
| RDE | rotating disc electrode |
| RRDE | rotating ring disc electrode |
| SEM | scanning electron microscopy |
| SFC | scanning flow cell |
| TEM | transmission electron microscopy |
| XAS | X-ray absorption spectroscopy |
| XPS | X-ray photoelectron spectroscopy |
| XRD | X-ray diffraction |

## References


1. J. Murawski, S. B. Scott, R. Rao, K. Rigg, C. Zalitis, J. Stevens, J. Sharman, G. Hinds, I. E. L. Stephens, *Johnson Matthey Technol. Rev.*, 2024, **68**, (1), 117
2. R. Chen, C. Yang, W. Cai, H.-Y. Wang, J. Miao, L. Zhang, S. Chen, B. Liu, *ACS Energy Lett.*, 2017, **2**, (5), 1070
3. M. A. Bird, S. E. Goodwin, D. A. Walsh, *ACS Appl. Mater. Interfaces*, 2020, **12**, (18), 20500
4. H. Yu, L. Bonville, J. Jankovic, R. Maric, *Appl. Catal. B: Environ.*, 2020, **260**, 118194
5. S. M. Alia, N. Danilovic, *Front. Energy Res.*, 2022, **10**, 857663
6. O. Kasian, J.-P. Grote, S. Geiger, S. Cherevko, K. J. J. Mayrhofer, *Angew. Chem. Int. Ed.*, 2018, **57**, (9), 2488
7. S. M. Alia, G. C. Anderson, *J. Electrochem. Soc.*, 2019, **166**, (4), F282
8. P. J. Petzoldt, J. T. H. Kwan, A. Bonakdarpour, D. P. Wilkinson, *J. Electrochem. Soc.*, 2021, **168**, (2), 026507
9. C. Spöri, C. Brand, M. Kroschel, P. Strasser, *J. Electrochem. Soc.*, 2021, **168**, (3), 034508
10. C. Wei, R. R. Rao, J. Peng, B. Huang, I. E. L. Stephens, M. Risch, Z. J. Xu, Y. Shao-Horn, *Adv. Mater.*, 2019, **31**, (31), 1806296
11. B. Seger, K. Vinodgopal, P. V. Kamat, *Langmuir*, 2007, **23**, (10), 5471
12. K. D. Kreuer, M. Ise, A. Fuchs, J. Maier, *Le J. Phys. IV France*, 2000, **10**, (7), 279
13. J. A. Arminio-Ravelo, A. W. Jensen, K. D. Jensen, J. Quinson, M. Escudero-Escribano, *ChemPhysChem*, 2019, **20**, (22), 2956
14. J. Knöppel, M. Möckl, D. Escalera-López, K. Stojanovski, M. Bierling, T. Böhm, S. Thiele, M. Rzepka, S. Cherevko, *Nat. Commun.*, 2021, **12**, 2231
15. S. Geiger, O. Kasian, M. Ledendecker, E. Pizzutilo, A. M. Mingers, W. T. Fu, O. Diaz-Morales, Z. Li, T. Oellers, L. Fruchter, A. Ludwig, K. J. J. Mayrhofer, M. T. M. Koper, S. Cherevko, *Nat. Catal.*, 2018, **1**, (7), 508
16. M. F. Tovini, A. Hartig-Weiß, H. A. Gasteiger, H. A. El-Sayed, *J. Electrochem. Soc.*, 2021, **168**, (1), 014512

17. M. J. N. Pourbaix, J. Van Muylde, N. de Zoubov, *Platinum Metals Rev.*, 1959, **3**, (3), 100
18. X. Peng, P. Satjaritanun, Z. Taie, L. Wiles, A. Keane, C. Capuano, I. V. Zenyuk, N. Danilovic, *Adv. Sci.*, 2021, **8**, (21), 2102950
19. S. B. Scott, R. R. Rao, C. Moon, J. E. Sørensen, J. Kibsgaard, Y. Shao-Horn, I. Chorkendorff, *Energy Environ. Sci.*, 2022, **15**, (5), 1977
20. A. C. Garcia, M. T. M. Koper, *ACS Catal.*, 2018, **8**, (10), 9359
21. A. Hartig-Weiss, M. F. Tovini, H. A. Gasteiger, H. A. El-Sayed, *ACS Appl. Energy Mater.*, 2020, **3**, (11), 10323
22. G. Papakonstantinou, I. Spanos, A. P. Dam, R. Schlögl, K. Sundmacher, *Phys. Chem. Chem. Phys.*, 2022, **24**, (23), 14579
23. H. A. El-Sayed, A. Weiß, L. F. Olbrich, G. P. Putro, H. A. Gasteiger, *J. Electrochem. Soc.*, 2019, **166**, (8), F458
24. T. Ioroi, T. Nagai, Z. Siroma, K. Yasuda, *Int. J. Hydrogen Energy*, 2022, **47**, (91), 38506
25. S. Czioska, K. Ehelebe, J. Geppert, D. Escalera-López, A. Boubnov, E. Saraçi, B. Mayerhöfer, U. Krewer, S. Cherevko, J.-D. Grunwaldt, *ChemElectroChem*, 2022, **9**, (19), e202200514
26. S. Czioska, A. Boubnov, D. Escalera-López, J. Geppert, A. Zagalskaya, P. Röse, E. Saraçi, V. Alexandrov, U. Krewer, S. Cherevko, J.-D. Grunwaldt, *ACS Catal.*, 2021, **11**, (15), 10043
27. S. Geiger, O. Kasian, A. M. Mingers, S. S. Nicley, K. Haenen, K. J. J. Mayrhofer, S. Cherevko, *ChemSusChem*, 2017, **10**, (21), 4140
28. J. Edgington, A. Deberghes, L. C. Seitz, *ACS Appl. Energy Mater.*, 2022, **5**, (10), 12206
29. Y. Yi, G. Weinberg, M. Prenzel, M. Greiner, S. Heumann, S. Becker, R. Schlögl, *Catal. Today*, 2017, **295**, 32
30. Y.-R. Zheng, J. Vernieres, Z. Wang, K. Zhang, D. Hochfilzer, K. Krempl, T.-W. Liao, F. Presel, T. Altantzis, J. Fatermans, S. B. Scott, N. M. Secher, C. Moon, P. Liu, S. Bals, S. Van Aert, A. Cao, M. Anand, J. K. Nørskov, J. Kibsgaard, I. Chorkendorff, *Nat. Energy*, 2022, **7**, (1), 55
31. N. Trogisch, M. Koch, E. N. El Sawy, H. A. El-Sayed, *ACS Catal.*, 2022, **12**, (21), 13715
32. C. Wei, S. Sun, D. Mandler, X. Wang, S. Z. Qiao, Z. J. Xu, *Chem. Soc. Rev.*, 2019, **48**, (9), 2518
33. S. Jung, C. C. L. McCrory, I. M. Ferrer, J. C. Peters, T. F. Jaramillo, *J. Mater. Chem. A*, 2016, **4**, (8), 3068
34. T. Reier, M. Oezaslan, P. Strasser, *ACS Catal.*, 2012, **2**, (8), 1765
35. R. Woods, *J. Electroanal. Chem. Interfacial Electrochem.*, 1974, **49**, (2), 217
36. S. M. Alia, K. E. Hurst, S. S. Kocha, B. S. Pivovar, *J. Electrochem. Soc.*, 2016, **163**, (11), F3051
37. W. Q. Zaman, W. Sun, M. Tariq, Z. Zhou, U. Farooq, Z. Abbas, L. Cao, J. Yang, *Appl. Catal. B: Environ.*, 2019, **244**, 295
38. M. E. G. Lyons, S. Floquet, *Phys. Chem. Chem. Phys.*, 2011, **13**, (12), 5314
39. K. A. Stoerzinger, L. Qiao, M. D. Biegalski, Y. Shao-Horn, *J. Phys. Chem. Lett.*, 2014, **5**, (10), 1636
40. S. Watzele, A. S. Bandarenka, *Electroanalysis*, 2016, **28**, (10), 2394
41. S. Watzele, P. Hauenstein, Y. Liang, S. Xue, J. Fichtner, B. Garlyyev, D. Scieszka, F. Claudel, F. Maillard, A. S. Bandarenka, *ACS Catal.*, 2019, **9**, (10), 9222
42. A. Lončar, P. Jovanovič, N. Hodnik, M. Gaberšček, *J. Electrochem. Soc.*, 2023, **170**, (4), 044504
43. S. P. Kounaves, J. Buffle, *J. Electrochem. Soc.*, 1986, **133**, (12), 2495
44. C. M. Zalitis, D. Kramer, A. R. Kucernak, *Phys. Chem. Chem. Phys.*, 2013, **15**, (12), 4329
45. M. Inaba, A. W. Jensen, G. W. Sievers, M. Escudero-Escribano, A. Zana, M. Arenz, *Energy Environ. Sci.*, 2018, **11**, (4), 988
46. A. Hrnjić, F. Ruiz-Zepeda, M. Gaberšček, M. Bele, L. Suhadolnik, N. Hodnik, P. Jovanovič, *J. Electrochem. Soc.*, 2020, **167**, (16), 166501
47. S. Watzele, Y. Liang, A. S. Bandarenka, *ACS Appl. Energy Mater.*, 2018, **1**, (8), 4196
48. C. Locatelli, A. Minguzzi, A. Vertova, P. Cava, S. Rondinini, *Anal. Chem.*, 2011, **83**, (7), 2819
49. A. Minguzzi, C. Locatelli, O. Lugaresi, A. Vertova, S. Rondinini, *Electrochim. Acta*, 2013, **114**, 637
50. R. A. Rincón, A. Battistel, E. Ventosa, X. Chen, M. Nebel, W. Schuhmann, *ChemSusChem*, 2015, **8**, (3), 560
51. M. Kroschel, A. Bonakdarpour, J. T. H. Kwan, P. Strasser, D. P. Wilkinson, *Electrochim. Acta*, 2019, **317**, 722
52. D. Siegmund, S. Metz, V. Peinecke, T. E. Warner, C. Cremers, A. Grevé, T. Smolinka, D. Segets, U.-P. Apfel, *JACS Au*, 2021, **1**, (5), 527
53. M. Bernt, H. A. Gasteiger, *J. Electrochem. Soc.*, 2016, **163**, (11), F3179
54. M. Möckl, M. F. Ernst, M. Kornherr, F. Allebrod, M. Bernt, J. Byrknes, C. Eickes, C. Gebauer, A. Moskovtseva, H. A. Gasteiger, *J. Electrochem. Soc.*, 2022, **169**, (6), 064505
55. M. P. Browne, J. Dodwell, F. Novotny, S. Jaśkaniec, P. R. Shearing, V. Nicolosi, D. J. L. Brett, M. Pumera, *J. Mater. Chem. A*, 2021, **9**, (14), 9113
56. G. Tsotridis, A. Pilenga, "EU Harmonized Protocols for Testing of Low Temperature Water Electrolysis", JRC Technical Report No. JRC122565, European

 

Commission, Petten, The Netherlands, 2021, 171 pp

57. S. M. Alia, K. S. Reeves, H. Yu, J. Park, N. Kariuki, A. J. Kropf, D. J. Myers, D. A. Cullen, *J. Electrochem. Soc.*, 2022, **169**, (5), 054517
58. M. Clapp, C. M. Zalitis, M. Ryan, *Catal. Today*, 2023, **420**, 114140
59. M. Bernt, A. Siebel, H. A. Gasteiger, *J. Electrochem. Soc.*, 2018, **165**, (5), F305
60. A. Nilsson, I. Stephens, 'Sustainable $N_2$ Reduction', in "Research Needs Towards Sustainable Production of Fuels and Chemicals", eds. A. Latimer, C. F. Dickens, Section 5, Energy-X, San Juan, Puerto Rico, 2019, pp. 49–59
61. S. B. Scott, J. E. Sørensen, R. R. Rao, C. Moon, J. Kibsgaard, Y. Shao-Horn, I. Chorkendorff, *Energy Environ. Sci.*, 2022, **15**, (5), 1988

## The Authors

James Murawski graduated from the University of Southampton in 2018, UK, with a Master's degree in Chemistry. He is currently finishing PhD studies at Imperial College London in the area of acid based OER catalyst stability and degradation for PEM water electrolyser applications.

Soren B. Scott is a Danish-American researcher focused on electrocatalysis and its central role in the green transition. He has a PhD in Physics from the Technical University of Denmark and is presently a postdoctoral fellow based in Ifan Stephens' group at Imperial College London with funding from the Iberdrola Foundation's Energy for Future program.

Reshma R. Rao is a Royal Academy of Engineering Research Fellow in the Department of Materials, Imperial College London. Her research focuses on understanding reactivity at solid-liquid interfaces using *operando* spectroscopic techniques to design more active, stable and selective catalysts for electrochemical energy conversion technologies.

Katie Rigg graduated from the University of Leeds, UK, in 2018 with a MNatSci in Maths and Chemistry. She began her research at Johnson Matthey working on oxygen evolution and $CO_2$ reduction catalysis and now specialises in PEM water electrolysis focusing on CCM testing and anode layer characterisation.

Chris Zalitis is an electrochemistry group lead in the Hydrogen Technologies team at Johnson Matthey focusing on CCM development for hydrogen electrolysers. In 2008 he earned his Master of Chemistry degree at the University of Southampton and in 2012 he earned his PhD at Imperial College London on the topic of electrocatalysis of fuel cell reactions.

 

Jamie Stevens is water electrolysis research group leader at Johnson Matthey, Sonning Common, UK.

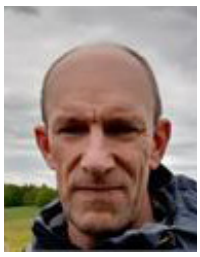

Jonathan Sharman runs the Hydrogen Technologies research groups at Johnson Matthey encompassing fuel cells, electrolysers and ion conducting membranes. His research interests cover the electrocatalysis within these systems, the structure-property relationships within CCMs and the electrochemical and *ex situ* characterisation techniques that probe the related material sets.

Gareth Hinds is NPL Fellow and Science Area Leader in the Electrochemistry Group at the National Physical Laboratory in Teddington, UK. His main research interests lie in the development of novel *in situ* diagnostic techniques and standard test methods for assessment of corrosion and material degradation in energy applications.

Ifan Stephens' research aims to enable the large-scale electrochemical conversion of renewable electricity and abundant feedstocks ($H_2O$, $N_2$, $CO_2$) to fuels and valuable chemicals (e.g. $H_2$, $NH_3$, $C_2H_4$). His focus is on the catalysis. Stephens is the recipient of numerous awards, including the ERC Consolidator Grant, Clarivate Highly Cited Researcher, MIT's Peabody Visiting Associate Professorship and RSC's John Jeyes prize.